Research Square

Preprints are preliminary reports that have not undergone peer review.
They should not be considered conclusive, used to inform clinical practice,
or referenced by the media as validated information.

Somatostatin receptor 2 expression in relation to ^{68}Ga-DOTATOC and ^{18}F-FDG PET/CT uptake in high-grade neuroendocrine neoplasms: a retrospective single-centre study

Dennis Truong

dennis.truong@ki.se

KI MMK: Karolinska Institutet Institutionen for molekylar medicin och kirurgi https://orcid.org/0009-0005-0049-2732

Zandra Ankers

Karolinska Institutet Institutionen for onkologi-patologi

Joachim N. Nilsson

KI MMK: Karolinska Institutet Institutionen for molekylar medicin och kirurgi

Renske Altena

Karolinska Institutet Institutionen for onkologi-patologi

Adam Stenman

KI MMK: Karolinska Institutet Institutionen for molekylar medicin och kirurgi

Hanna M. Ingelman-Sundberg

KI MMK: Karolinska Institutet Institutionen for molekylar medicin och kirurgi

Olle Kämpe

Karolinska Institutet Institutionen for Medicin Solna

C. Christofer Juhlin

Karolinska Institutet Institutionen for onkologi-patologi

Anna Kistner

KI MMK: Karolinska Institutet Institutionen for molekylar medicin och kirurgi

Research Article

Keywords: neuroendocrine cancer, somatostatin receptor 2, ^{68}Ga-DOTATOC PET/CT, ^{18}F-FDG PET/CT, immunohistochemistry, RRID:AB_3695715

Posted Date: November 23rd, 2026

DOI: https://doi.org/10.21203/rs.3.rs-11571097/v1

License: This work is licensed under a Creative Commons Attribution 4.0 International License.
Read Full License

Somatostatin receptor 2 expression in relation to ^{68}Ga-DOTATOC and ^{18}F-FDG PET/CT uptake in high-grade neuroendocrine neoplasms: a retrospective single-centre study

Dennis Truong[1,2], Zandra Ankers[3,4], Joachim N. Nilsson[1,2], Renske Altena[3], Adam Stenman[2,5], Hanna M. Ingelman-Sundberg[2,6], Olle Kämpe[7,8], C. Christofer Juhlin[3,4], Anna Kistner[1,2]

1. Department of Nuclear Medicine and Medical Physics, Karolinska University Hospital, Stockholm, Sweden

2. Department of Molecular Medicine and Surgery, Karolinska Institutet, Stockholm, Sweden

3. Department of Oncology-Pathology, Karolinska Institutet, Stockholm, Sweden

4. Department of Clinical Pathology and Cancer Diagnostics, Karolinska University Hospital, Stockholm, Sweden

5. Department of Breast, Endocrine Tumors and Sarcoma, Karolinska University Hospital, Stockholm, Sweden

6. Department of Oncology, Karolinska University Hospital, Stockholm, Sweden

7. Department of Medicine, Karolinska Institutet, Stockholm, Sweden

8. Department of Endocrinology, Karolinska University Hospital, Stockholm, Sweden

Correspondence to:

Dennis Truong

Mail: Dennis.Truong@ki.se

Phone: +46 73 886 51 92

Nuclear Medicine and Medical Physics,

Karolinska University Hospital,

Stockholm, Sweden

Abbreviations

^{68}Ga-DOTATOC – gallium-68 DOTA-Tyr^{3}-octreotide

^{177}Lu-DOTATATE – lutetium-177 DOTA-Tyr^{3}-octreotate

^{18}F-FDG – fluorine-18 fluorodeoxyglucose

5-HIAA – 5-hydroxyindoleacetic acid

CA 19-9 – carbohydrate antigen 19-9

CA-125 – cancer antigen 125

CAPTEM – capecitabine and temozolomide

CEA – carcinoembryonic antigen

CI – confidence interval

CT – computed tomography

CUP – carcinoma of unknown primary

FDG – fluorodeoxyglucose

FOLFIRI – 5-fluorouracil, leucovorin and irinotecan

GEP-NEN – gastroenteropancreatic neuroendocrine neoplasm

GI – gastrointestinal

IHC – immunohistochemistry

IQR – interquartile range

MIP – maximum intensity projection

NEC – neuroendocrine carcinoma

NEN – neuroendocrine neoplasm

NET – neuroendocrine tumour

NET G3 – grade 3 neuroendocrine tumour

NPV – negative predictive value

PD-L1 – programmed death-ligand 1

PET – positron emission tomography

PPV – positive predictive value

PRRT – peptide receptor radionuclide therapy

RB1 – retinoblastoma 1

SNOMED – Systematized Nomenclature of Medicine

SSTR – somatostatin receptor

SSTR2 – somatostatin receptor subtype 2

SUV – standardized uptake value

SUVmax – maximum standardized uptake value

TLR – tumour-to-liver ratio

WHO – World Health Organization

Abstract

Background: High-grade neuroendocrine neoplasms (NEN), including grade 3 neuroendocrine tumours (NETG3) and neuroendocrine carcinomas (NEC) are often assumed to lose somatostatin receptor (SSTR) expression. Our study explores the relationship between SSTR2 immunohistochemistry (IHC), ^{68}Ga-DOTATOC and ^{18}F-FDG PET/CT uptake, Ki-67 and overall survival.

Methods: Retrospective single-centre study of 48 patients (NETG3, n = 13; NEC, n = 35) diagnosed 2021–2024. The patients represent a subset of a previously described cohort, with published histopathological and clinical data now correlated with radiological findings. 57 PET/CT scans (^{68}Ga-DOTATOC, n = 34; ^{18}F-FDG, n = 23) were re-analyzed. DOTATOC uptake was graded by Krenning score and FDG avidity was defined as tumour-to-liver ratio ≥1.0. SSTR2 IHC was available for 34 patients and used as the index test.

Results: Immunohistochemistry was available for 34 of 48 patients and SSTR2 was expressed in 26/34 tumours (76%). IHC status was significantly associated with a higher Krenning score (p = 0.007, Cochran–Armitage trend test). At Krenning score ≥2, IHC had 93% sensitivity, 50% specificity, 74% positive predictive value (PPV) and 83% negative predictive value (NPV) and at Krenning score ≥3, sensitivity was 100%, specificity 43%, PPV 58% and NPV 100%. Of 15 FDG-avid patients with IHC, 13 (87%) were IHC-positive. Seven of nine dual-tracer patients had a high uptake on both tracers. Uptake of either tracer correlated with Ki-67 or overall survival.

Conclusions: SSTR2 expression assessed by immunohistochemistry was significantly associated with ^{68}Ga-DOTATOC uptake. Positive SSTR2 expression may warrant ^{68}Ga-DOTATOC PET imaging even in patients with high-grade NEN. Furthermore, positive SSTR2 expression and corresponding ^{68}Ga-DOTATOC uptake may identify patients with high-grade NEN who could potentially benefit from peptide receptor radionuclide therapy (PRRT) with ^{177}Lu-DOTATATE (Lutathera). FDG avidity often coexisted with at least partial SSTR2 expression. Prospective interventional studies incorporating lesion-matched analyses are warranted to further validate these findings.

Keywords: neuroendocrine cancer, somatostatin receptor 2, ^{68}Ga-DOTATOC PET/CT, ^{18}F-FDG PET/CT, immunohistochemistry, RRID:AB_3695715

Introduction

Neuroendocrine neoplasms (NEN) are a heterogeneous group of rare malignancies divided into well-differentiated neuroendocrine tumours (NET), which typically exhibit more indolent behavior, and poorly differentiated neuroendocrine carcinomas (NEC), which are known for their aggressive clinical course. According to the 2022 WHO classification, this division relies heavily on tumour morphology, mitotic count and the Ki-67 proliferation index. (1) NET can be further divided into grades G1 through G3 (with G3 defined as a mitotic count > 20/ 2 mm2 and/or Ki-67 >20%). NEC inherently display high-grade histological features alongside a Ki-67 index exceeding 20% (1). NET grade 3 is defined by high proliferation but preserved differentiation, with median overall survival in metastatic disease ranging from 19 to 99 months, whereas NEC, characterized by Ki-67 > 20% and poor differentiation, has a median survival of about 12 months despite chemotherapy (2,3). Large series indicate particularly poor outcomes for pancreatic NEC, with median survival as low as 6 months (4).

Molecular imaging plays an important role in the characterization and clinical management of these neoplasms. Historically, somatostatin-receptor (SSTR) PET imaging, such as ^{68}Ga-DOTATOC, has been the standard of care for well-differentiated NETs due to their consistent SSTR expression (5). High uptake correlates with somatostatin receptor expression and longer progression-free survival (6). On the other hand, ^{18}F-FDG PET/CT is utilized for high-grade NET and NEC, as highly proliferative neoplasms often show high FDG-uptake reflecting their increased glucose metabolism and presumed lack of somatostatin receptors. Low standardized uptake value (SUVmax) on ^{68}Ga-somatostatin receptor PET/CT combined with high FDG uptake correlates with higher Ki67, more aggressive biology and poorer prognosis. (7,8) However, emerging data indicates a more complex picture; that there is a

120 considerable number of NETG3/NEC cases with high proliferation index that maintains at
121 least partial immunohistochemical SSTR2 expression (9).

122 This unexpected SSTR expression in NETG3/NEC carries significant therapeutic
123 implications. In the randomized NETTER-2 trial, first-line ^{177}Lu-DOTATATE peptide
124 receptor radionuclide therapy (PRRT) prolonged progression-free survival in patients with
125 SSTR-positive, well-differentiated grade 2–3 gastroenteropancreatic NET (19), and
126 retrospective series suggest that selected patients with NETG3 or NEC and sufficient SSTR
127 expression may also benefit (10).

128 Because treatment options for high-grade NEN are limited, and most patients experience only
129 a rather limited and short-lived response to chemotherapy with potentially severe side-effects,
130 there is a need to find alternative therapeutic approaches. Identifying which patients with
131 advanced, high-grade NEN possess these targetable receptors can therefore play a crucial role
132 in guiding and optimizing personalized treatment strategies.

133 To address this knowledge gap, this retrospective study aimed to investigate the relationship
134 between tracer uptake on ^{68}Ga-DOTATOC PET/CT and ^{18}F-FDG PET/CT to tumour SSTR2
135 expression assessed by immunohistochemistry in a well-defined cohort of patients with
136 NETG3 and NEC. Our cohort comprises a subgroup of a previously established and collected
137 population described by Ankers et al. (9), which we now investigate in relation to radiological
138 findings.

139 We further aimed to evaluate whether radiological isotope uptake was associated with
140 primary tumour origin, molecular characteristics, and overall survival.

Methods

This retrospective, single-center study was conducted at the Karolinska University Hospital and approved by the Swedish Ethical Review Authority (approval number 2025-07237-01). Patients were identified through electronic medical records using Systematized Nomenclature of Medicine (SNOMED) codes for NET and NEC. A pathologist then reviewed the pathology reports for all identified cases to confirm classification as NETG3/ NEC, this yielded in 87 patients diagnosed between January 2021 and July 2024. Our cohort represents an imaging-specific subgroup of this larger population previously described by Ankers et al. (9).

In Figure 1, the flowchart of the patient cohort is shown. Patients were included if they had undergone ^{18}F-FDG PET/CT, ^{68}Ga-DOTATOC PET/CT, or both. Exclusion criteria were lack of PET/CT imaging (n=37). Two patients were excluded because the PET examinations had been performed at another hospital, and some data was missing for central evaluation. The final study cohort comprised 48 patients (NET grade 3, n=13; NEC, n=35). The data shared with the earlier publication include baseline clinicopathological characteristics and SSTR2 immunohistochemistry (IHC) findings. The novel aspects of the present study are imaging analysis and its correlation with SSTR2 IHC expression and overall survival.

Image Acquisition

All PET/CT imaging was performed according to routine clinical protocols, with minor changes over the study period. ^{18}F-FDG was administered at 3 MBq/kg after ≥6 h fasting. ^{68}Ga-DOTATOC was given at 100 MBq (BMI <35 kg/m²) or 150 MBq (BMI ≥35 kg/m²). Images were acquired from skull base to upper thigh ~60 min post-injection on a Siemens Biograph mCT (Siemens Healthineers, Erlangen, Germany; continuous bed motion, 1.2 mm/s) or a GE Discovery MI (GE HealthCare, Waukesha, WI, USA; 2.5 min/bed). Reconstruction uses OSEM with TOF and PSF modelling (mCT: 2 iterations, 21 subsets, 400

× 400 matrix, 5-mm Gaussian filter; Discovery MI: 3 iterations, 17 subsets, 256 × 256 matrix, 5.5-mm Gaussian and heavy z-axis filter). Low-dose CT was used for attenuation correction, with correction for scatter, randoms, and decay.

Immunohistochemistry

Immunohistochemical staining for somatostatin receptor 2 (SSTR2) was performed as part of routine clinical diagnostics using a VENTANA BenchMark automated staining platform (Roche, Basel, Switzerland). Tissue sections (4 µm thick) were mounted on Superfrost Plus slides. Heat-induced antigen retrieval was performed using Cell Conditioning 1 (CC1) at 100°C for 32 min, followed by incubation with an anti-SSTR2 antibody clone EP149 (Cell Marque Cat#486R, RRID:AB_3695715), for 32 min. Sections were counterstained with Hematoxylin II for 8 min, followed by Bluing Reagent for 4 min. External control tissues were mounted on the same slide as the tumor sections and evaluated alongside them. Normal pancreatic tissue, with pancreatic islet cells serving as positive control, and normal colon and lymph node tissues serving as negative controls were included.

SSTR2 immunoreactivity was evaluated using a three-tier grading system consistent with the primary histopathological analysis by Ankers et al (9). The classification was based on the assessment of SSTR2 expression on tissue from 34 patients. Biopsies from metastases in 19 (liver, n = 18; lymph node, n = 1), biopsies from the primary tumour in 6, surgical specimens of metastases in 5 (lymph node, n = 2; ovary, thyroid and brain, n = 1 each) and surgical specimens of the primary tumour in 4 (including regional lymph node metastases or local recurrence in 2).

SSTR2 expression was assessed by an experienced endocrine pathologist (C.C.J.), blinded to the PET findings, and scored as the percentage of tumour cells showing membranous staining (IHC-score).

- **IHC-score 0 (Negative):** <5% of tumour cells stained.
- **IHC- score 1 (Partially Positive):** 5–74% of tumour cells stained.
- **IHC-score 2 (Positive):** ≥75% of tumour cells stained.

For the purposes of correlation with PET/CT imaging, tumours were considered SSTR2-positive if they exhibited IHC-score 1 or IHC-score 2 expressions. (9)

Data Collection

Patient demographics, circulating biomarkers when available (Chromogranin A, 5-HIAA, CEA, CA 19-9, and CA-125), and histopathological parameters (Ki-67 index, SSTR2 immunohistochemistry, and mutational status, p53, RB1 and PD-L1 expression) were extracted from medical records. Overall survival data was verified using the Swedish Population Register, with 8 January 2026 as the end of follow-up.

Image Acquisition and Analysis

PET/CT examinations performed between May 2017 and March 2025 were retrospectively analysed. Four patients had an initial NET G2 diagnosis that later transformed to NET G3/NEC during study inclusion time. Three of them underwent PET imaging before 2021, and these scans were included. Routine clinical protocols at our institution generally have somewhat shifted over the years during which the material was collected. ^{68}Ga-DOTATOC PET/CT is typically performed at progression to evaluate treatment options such as surgery or ^{177}Lu-DOTATATE.

All imaging studies were independently re-analyzed by two radiologists (AK, DT) with subspecialty training in nuclear medicine. The analyses were performed blinded for information about patient and treatment. Primary tumour location and volume were analyzed. SUVmax was measured for both ^{18}F-FDG and ^{68}Ga-DOTATOC scans using HERMES

Affinity software (version 5.0). For each patient, the lesion with the highest SUVmax, most often a liver metastasis primary tumour or both if available, was used for analysis. This lesion was therefore not necessarily the same lesion assessed by IHC (Additional file 1: Supplemental Table 1).

For ^{68}Ga-DOTATOC PET/CT, tumour uptake of the lesion with highest uptake was used and evaluated and determined according to the Krenning Score Criteria (11,12). In patients with extensive hepatic tumour burden, the reference region was placed in an area of visually uninvolved liver tissue to minimize contamination by tumour uptake and its potential impact on TLR and Krenning scores. High ^{18}F-FDG uptake was defined as a tumour-to-liver ratio (TLR) ≥1.0, calculated as lesion SUVmax divided by SUVmax of normal liver parenchyma. This threshold corresponds to uptake at the upper limit of a Krenning score 2 (equal to liver) or higher (Krenning score 3–4)

Krenning score Criteria

- Score 0 – No uptake
- Score 1 – Very low uptake
- Score 2 – Uptake less than or equal to that of the liver
- Score 3 – Uptake greater than the liver
- Score 4 – Uptake greater than that of the spleen

For the subgroup of patients who underwent both ^{18}F-FDG and ^{68}Ga-DOTATOC PET/CT (n = 9), a dual-tracer evaluation was performed. SSTR positivity was defined as a Krenning score ≥2 and high FDG uptake as a TLR ≥1.0. A Krenning score ≥3 (uptake greater than liver) was additionally used as the clinically relevant threshold for PRRT eligibility.

- Double-positive (SSTR+/FDG+): Krenning score ≥2 and TLR ≥1.0
- Discordant SSTR-negative (SSTR−/FDG+): Krenning score 0–1 and TLR ≥1.**0**
- Discordant FDG-negative (SSTR+/FDG−): Krenning score ≥2 and TLR <1.0
- Double-negative (SSTR−/FDG−): Krenning score 0–1 and TLR <1.0

Statistical Analysis

Categorical variables were compared using Fisher's exact test. The trend between SSTR2 IHC status and ^{68}Ga-DOTATOC Krenning score category was assessed using the Cochran–Armitage trend test. To reflect clinical practice, in which IHC is usually available before PET imaging, SSTR2 IHC was used as the index test and ^{68}Ga-DOTATOC PET/CT as the reference standard. As PRRT eligibility is based on SSTR-PET uptake, the reverse analysis is provided in Additional file 1: Supplemental Figure 2. Sensitivity, specificity, PPV and NPV were calculated with 95% confidence intervals using the Wilson score method. Correlations between SUVmax and SSTR2 IHC score or Ki-67 index were assessed using Spearman's rank correlation, as SUVmax values were not normally distributed. Interobserver agreement for SUVmax was assessed using Bland–Altman analysis. Overall survival was calculated from the date of diagnosis to death or censoring at end of follow-up (8 January 2026) and analysed using the Kaplan–Meier method. A two-sided p-value of <0.05 was considered statistically significant. All statistical analyses and graphical representations were conducted using R version 4.6.0 (R Foundation for Statistical Computing, Vienna, Austria)

Results

A total of 48 patients with NETG3/NEC were included in the study. PET imaging findings were analyzed and correlated with clinical and histopathological data. Table 1 summarizes

patient demographics, tumour grade, histopathological characteristics, biochemical parameters and treatment regimens. Additional file 1: Supplemental Table 1 summarizes the biopsy or surgical speciment in relation to the lesion measured on ^{18}F-FDG and ^{68}Ga-DOATOC PET/CT.

The cohort exhibited a median age of 72 years (range 37-88) and comprised of 30 men (62.5%) and 18 women (37.5%).

Primary tumours were most frequently located in the pancreas (n=19; 40 %), followed by carcinomas of unknown primary (CUP) (n=9; 19 %) and the rectum (n=5; 10 %). At the time of imaging, distant metastases were commonly observed, occurring most commonly in the liver (n=35; 73 %), abdominal lymph nodes (n=29; 60 %), and bone (n=15; 31 %). Lung-intracranial- and adrenal metastases were less frequently present in the cohort (Table 1).

For 33 patients where the primary tumour was able to be identified, volumetric data was obtained. Median primary tumour volume was 30 ml, with an interquartile range (IQR) of 9.5 to 85 ml (range: 0.6–1138 ml).

Regarding histopathological grading, 35 patients were classified as having NEC (73%), while 13 patients (27%) had NETG3. The median Ki-67 proliferation index was for NETG3 28% (IQR:24-33), for NEC 80% (IQR 67.5-90).

SSTR2 immunohistochemistry was available for 34 patients (NEC, n = 22; NETG3, n = 12); of these, 14 (41%) demonstrated significant SSTR2 expression (IHC-score 2), 12 (35%) showed partial expression (IHC-score 1), and 8 (24%) were negative (IHC-score 0). The proportion of SSTR2-positive tumours (IHC-score 1–2) was similar in NEC and NETG3 (77% vs. 75%, p = 1.0).

PET/CT Imaging Tracer Uptake in Relation to IHC SSTR2 expression

Among the 48 patients, 57 PET/CT examinations were analyzed (^{18}F-FDG, n = 23; ^{68}Ga-DOTATOC, n = 34), and nine patients underwent both. Interobserver agreement is shown in Additional file 1: Supplemental Figure 1.

SSTR2 IHC was available for 25 of the 34 patients examined with ^{68}Ga-DOTATOC PET/CT. IHC status was significantly associated with Krenning score (p = 0.007, Cochran–Armitage trend test) (Figure 2, Figure 3A–B, Table 2). At Krenning score ≥2, IHC positivity had a sensitivity of 93%, specificity of 50%, PPV of 74% and NPV of 83%. At the PRRT-relevant threshold of Krenning score ≥3, sensitivity and NPV were both 100% (specificity 43%, PPV 58%). All 11 PET-positive patients were IHC-positive, and none of the six IHC-negative patients had a Krenning Score ≥3.

With ^{68}Ga-DOTATOC as the index test SSTR-uptake was associated with SSTR2 expression (p = 0.007). (Additional file 1: Supplemental Figure 2). At Krenning score ≥ 3, specificity and PPV reached 100%, but sensitivity decreased to 58%.

Within those who underwent ^{18}F-FDG PET/CT (n=23), 17 patients had available SSTR2 histopathology. High metabolic activity (TLR ≥ 1.0) was identified in 15 of these patients either in metastases or primary tumour, and 87% (13/15) retained SSTR2 expression (IHC-score 1-2), while only 13% (n=2) were SSTR2-negative (IHC-score =0). In the subgroup with low FDG uptake (TLR < 1.0, n=2), one patient was SSTR2-positive (IHC-score =1), and one was negative. SSTR2 status did not differ significantly between patients with high and low FDG uptake. With only two FDG-low patients, this comparison was underpowered to assess an inverse relationship; descriptively, however, high FDG uptake did not preclude SSTR2 expression. (Additional file 1: Supplemental Figure 3).

Among the group who underwent dual-tracer imaging (n=9), the majority (n=7) exhibited a Double Positive phenotype (SSTR+/FDG+). One patient (11%) showed a SSTR-/FDG-

(double negative) phenotype, while another (11%) demonstrated a discordant SSTR-/FDG+ phenotype. (Figure 4 and Additional file 1: Supplemental Figure 4).

In a couple of patients, the concordance between FDG and DOTATOC was heterogeneous, with uptake in some liver metastases but not in others (Additional file 1: Supplemental Figure 5). In Figure 5 the SSTR-/FDG+ patient is presented.

PET/CT Imaging Tracer Uptake in Relation to Ki-67 index

In Figure 6A–B, the tracer uptake in relation to Ki-67 index is plotted. No correlation was found between Ki-67 index and ^{68}Ga-DOTATOC SUVmax (Spearman $\rho = 0.05$, $p = 0.791$, $n = 34$) or ^{18}F-FDG SUVmax ($\rho = 0.15$, $p = 0.49$, $n = 23$) (Figure 6A–B).

Mortality and overall survival

The median survival time after NET grade 3 diagnosis or NEC was 20 (IQR 11-28) months (Table 1). Most patients in the cohort had died by the time of follow-up (n= 40/48, 83.3%). Overall survival in relation to tracer uptake categorised into Krenning Score (Additional file 1: Supplemental Figure 6A), into high versus low tracer uptake at ^{68}Ga-DOTATOC (Krenning score ≥3 vs <3) (Additional file 1: Supplemental Figure 6B), and in relation to SUVmax at ^{18}F-FDG-PET (Additional file 1: Supplemental Figure 6C) were calculated. No association between tracer uptake and overall survival was observed in either model ($p = 0.45$, $p = 0.25$ and $p = 0.82$ respectively).

[Table 1 near here]

Table 2. ^{68}Ga-DOTATOC Krenning score according to SSTR2 IHC score (n = 25)

SSTR2 IHC score	n	Krenning 0–1	Krenning 2	Krenning 3–4
0	6	5 (83%)	1 (17%)	0 (0%)
1	6	2 (33%)	1 (17%)	3 (50%)
2	13	3 (23%)	2 (15%)	8 (62%)

SSTR2 IHC score	n	Krenning 0–1	Krenning 2	Krenning 3–4
Diagnostic accuracy of IHC (score 1–2) for PET positivity		**Krenning ≥2**		**Krenning ≥3**
Sensitivity		93% (14/15; 70–99)		100% (11/11; 74–100)
Specificity		50% (5/10; 24–76)		43% (6/14; 21–67)
PPV		74% (14/19; 51–88)		58% (11/19; 36–77)
NPV		83% (5/6; 44–97)		100% (6/6; 61–100)
p (Fisher's exact test)		0.023		0.020

Values are % (n/N; 95% confidence interval). PPV, positive predictive value; NPV, negative predictive value.

Discussion

In this retrospective single-center study of patients with high-grade neuroendocrine neoplasms, including NETG3 and NEC, we evaluated the relationship between ^{68}Ga-DOTATOC uptake, ^{18}F-FDG uptake, tumour SSTR2 expression, and overall survival. Three observations are of particular interest. Firstly, SSTR2 expression assessed by immunohistochemistry was significantly associated with ^{68}Ga-DOTATOC uptake on PET/CT, suggesting that positive SSTR2 expression should prompt consideration of somatostatin receptor PET/CT even in patients with high-grade NEN. Viewed from the imaging perspective, all patients with high ^{68}Ga-DOTATOC uptake (Krenning score ≥3) were SSTR2-positive, whereas low uptake did not exclude SSTR2 expression. Secondly, high ^{18}F-FDG-uptake was frequent and was not significantly associated with loss of SSTR2 expression, although this comparison was underpowered. Third, despite the overall aggressive disease phenotype, neither SSTR-PET-CT uptake nor FDG-uptake was significantly associated with overall survival in this cohort.

The association between SSTR2 expression and ^{68}Ga-DOTATOC-uptake supports the use of SSTR-PET as a non-invasive marker of receptor expression in high-grade NEN. The positive predictive value (PPV) of 74% indicates that among NETG3/NEC individuals with an IHC-score of 1–2, 74% are identified with a Krenning score ≥2 on ^{68}Ga-DOTATOC. In our

cohort, all patients with high DOTATOC uptake and available immunohistochemistry demonstrated SSTR2 expression, whereas half of patients with low uptake retained SSTR2 expression. This discordance may reflect differences in how PET and histopathology assess tumour characteristics and the intra- and interlesional heterogeneity of high-grade NENs. (13) Therefore, low SSTR-PET uptake should not necessarily be interpreted as complete absence of SSTR2 expression.

In addition, several studies suggest a correlation between SSTR expression and the benefit of PRRT. Ambrosini et al. (15) reported better outcomes in patients with high baseline SUVs, and Kratochwil et al. (16) found that high pretherapy uptake in liver metastases predicted a good therapeutic response.

Another important finding was the absence of a significant inverse relationship between ^{18}F-FDG uptake and SSTR2 expression on immunohistochemistry. Among patients with available immunohistochemistry, 87% (13/15) of those with high FDG uptake retained SSTR2 expression. This suggests that high FDG avidity and preserved somatostatin receptor expression can coexist in high-grade NEN. ^{18}F-FDG and ^{68}Ga-DOTATOC PET/CT therefore appear to provide complementary rather than opposing information. FDG- reflects tumour metabolic activity, whereas ^{68}Ga-DOTATOC uptake reflects receptor expression and accessibility. The biology of high-grade NEN may thus be viewed as a spectrum rather than a rigid transition from SSTR-positive to FDG-positive disease (14). Despite the small sample size, our findings suggest that high FDG uptake should not discourage SSTR-PET imaging. Clinically PRRT eligibility is based on ^{68}Ga-DOTATOC uptake rather than immunohistochemical expression, our results support ^{68}Ga-DOTATOC PET assessment even in FDG-avid disease, although treatment response was not evaluated.

The dual-tracer subgroup supports this concept. Seven of nine patients demonstrated high uptake on both tracers. Chan et al. proposed the NETPET score, which summarizes dual-

tracer PET findings coupled to prognostic factors (14). In a multicenter study of 319 patients with metastatic gastroenteropancreatic (GEP)-NEN, the NETPET score provided prognostic information beyond histological grade, with SSTR-positive/FDG-negative disease associated with the most favourable survival and SSTR-negative/FDG-positive disease with the poorest outcomes (20). As grade 3 tumours made up only 15% of that cohort, the value of dual-tracer phenotyping in high-grade NEN remains to be established, which is one justification for the present study. (20). NETPET positivity is visually defined as uptake above background on dual-tracer PET scans performed within 90 days, while we used the most avid lesion to assess the Krenning score on ^{68}Ga-DOTATOC PET/CT and TLR on FDG PET/CT. We therefore did not perform a NETPET scoring or a survival analysis by NETPET score.

In our cohort undergoing ^{68}Ga-DOTATOC PET/CT 47% (16/34) of patients demonstrated a Krenning score of 3-4 and high SSTR-tracer expression on PET/CT. These findings contradict findings from a recently published small prospective study in which only 13 % showed a uniformly high Ga-DOTATOC uptake, corresponding to Krenning grades 3–4 (17).

No significant correlation was observed between the Ki-67 index and SUVmax on either ^{68}Ga-DOTATOC or ^{18}F-FDG PET/CT, potentially reflecting the limited sample size of our cohort (for ^{18}F-FDG).

We found no significant association between SSTR or FDG PET parameters and overall survival, in contrast to previous studies (18). This may reflect the small cohort, limited dual-tracer imaging, variable imaging intervals, and treatment heterogeneity, highlighting the need for further investigation in larger cohorts.

Several limitations should be acknowledged. The retrospective single-centre design and small sample size limit statistical power and generalisability, and introduce a risk of selection by indication, as patients referred for a given PET examination may represent a clinically

selected population. SSTR2 IHC was available only for a subset of patients owing to limited biopsy material. Tissue sampling and PET were not necessarily performed simultaneously, and intervening treatment may have altered receptor expression. Moreover, the lesions assessed by IHC and by PET SUVmax were not necessarily the same, and a biopsy represents a limited tissue sample whereas PET reflects whole-body disease; some PET/IHC discordance may therefore reflect inter- and intralesional heterogeneity rather than true biological discordance. SUVmax was measured on two PET systems with protocols that changed over the study period, which may affect quantitative comparability. The high prevalence of liver metastases may affect liver-referenced measurements; although liver uptake was measured in visually normal parenchyma, subtle tumour involvement cannot be excluded. Finally, the dual-tracer subgroup comprised only nine patients, who were selected because SSTR-directed treatment was being considered, so the high rate of dual-tracer positivity should not be considered representative of all patients with high-grade NEN.

Conclusion

In high-grade neuroendocrine neoplasms (NETG3/NEC), immunohistochemical SSTR2 expression correlated with ^{68}Ga-DOTATOC uptake. Elevated ^{18}F-FDG-uptake uptake did not necessarily indicate loss of SSTR2 expression. Consequently, FDG avidity should not exclude patients from ^{68}Ga-DOTATOC imaging or be interpreted as evidence of loss of SSTR expression on immunohistochemistry. Rather, ^{68}Ga-DOTATOC -PET and ^{18}F-FDG-PET provide complementary phenotypic information for the characterization of high-grade NEN. Furthermore, the presence of SSTR2 expression alongside ^{68}Ga-DOTATOC uptake may support consideration of ^{177}Lu-DOTATATE (Lutathera) therapy in selected patients with high-grade NEN. Prospective longitudinal interventional studies using standardized dual-

tracer imaging are warranted to determine whether combined molecular imaging can improve prognostic stratification and patient selection for SSTR-directed therapies.

Declarations

Ethics approval and consent to participate

This retrospective, single-center study was conducted at Karolinska University Hospital and was approved by the Swedish Ethical Review Authority (approval number 2025-07237-01). The ethical approval explicitly covered the retrospective study design and the use of patient data without obtaining individual informed consent. Accordingly, the requirement for informed consent was waived as part of the approved study protocol. The study was conducted in accordance with the principles of the Declaration of Helsinki.

Consent for publication

Not applicable.

Availability of data and materials

Data is available from the corresponding author upon reasonable written request.

Competing interests

The authors declare no conflicts of interest in relation to this work.

Funding

This study was supported by Karolinska Institutet and by the Research and Development Unit, Department of Nuclear Medicine, Karolinska University Hospital, Stockholm, Sweden.

Authors' contributions

Dennis Truong: Investigation, Formal analysis, Data curation, Visualization, Validation, Writing – original draft, project administration.

Anna Kistner: Conceptualization, Methodology, Data curation, Investigation, Validation, Supervision, Writing – review & editing, project administration.

C. Christofer Juhlin, Zandra Ankers: Investigation (SSTR2 immunohistochemistry), Resources, Writing – review & editing, Data curation

Joachim N. Nilsson: Writing – review & editing, Visualization

Renske Altena, Adam Stenman, Hanna M Ingelman-Sundberg, Olle Kämpe: Writing – review & editing.

All authors approved the final manuscript.

Acknowledgements

No additional acknowledgements.

References

1. Rindi G, Mete O, Uccella S, Basturk O, La Rosa S, Brosens LAA, et al. Overview of the 2022 WHO Classification of Neuroendocrine Neoplasms. Endocr Pathol. 2022 Mar 16;33(1):115–54. doi:10.1007/s12022-022-09708-2

2. Boutin M, Mathews A, Badesha J, Paul A, Safro M, Gill S, et al. Well-Differentiated Grade 3 Neuroendocrine Tumors. Pancreas. 2022 Aug;51(7):756–62. doi:10.1097/MPA.0000000000002100

3. Pavel M, Öberg K, Falconi M, Krenning EP, Sundin A, Perren A, et al. Gastroenteropancreatic neuroendocrine neoplasms: ESMO Clinical Practice Guidelines for diagnosis, treatment and follow-up. Annals of Oncology. 2020 Jul;31(7):844–60. doi:10.1016/j.annonc.2020.03.304

4. Alese OB, Jiang R, Shaib W, Wu C, Akce M, Behera M, et al. High-Grade Gastrointestinal Neuroendocrine Carcinoma Management and Outcomes: A National Cancer

462 Database Study. Oncologist. 2020 May 1;25(5):e877–e877. doi:10.1634/theoncologist.2020-
463 0135

464 5. Barrio M, Czernin J, Fanti S, Ambrosini V, Binse I, Du L, et al. The Impact of
465 Somatostatin Receptor–Directed PET/CT on the Management of Patients with
466 Neuroendocrine Tumor: A Systematic Review and Meta-Analysis. Journal of Nuclear
467 Medicine. 2017 May;58(5):756–61. doi:10.2967/jnumed.116.185587

468 6. Carlsen EA, Johnbeck CB, Binderup T, Loft M, Pfeifer A, Mortensen J, et al. Cu-
469 DOTATATE PET/CT and Prediction of Overall and Progression-Free Survival in Patients
470 with Neuroendocrine Neoplasms. Journal of Nuclear Medicine. 2020 Oct;61(10):1491–7.
471 doi:10.2967/jnumed.119.240143

472 7. Karfis I, Marin G, Levillain H, Drisis S, Muteganya R, Critchi G, et al. Prognostic
473 value of a three-scale grading system based on combining molecular imaging with ^{68}Ga-
474 DOTATATE and ^{18}F-FDG PET/CT in patients with metastatic gastroenteropancreatic
475 neuroendocrine neoplasias. Oncotarget. 2020 Feb 11;11(6):589–99.
476 doi:10.18632/oncotarget.27460

477 8. Lee H, Nakamoto R, Moore SE, Pantel AR, Eads JR, Aparici CM, et al. Combined
478 Quantification of ^{18}F-FDG and ^{68}Ga-DOTATATE PET/CT for Prognosis in High-Grade
479 Gastroenteropancreatic Neuroendocrine Neoplasms. Acad Radiol. 2022 Sep;29(9):1308–16.
480 doi:10.1016/j.acra.2021.10.004

481 9. Ankers Z, Hellgren LS, Stenman A, Zedenius J, Juhlin CC. Distinguishing
482 neuroendocrine tumor grade 3 from neuroendocrine carcinoma in gastroenteropancreatic
483 high-grade neoplasms. Endocrine Oncology. 2025 Dec 9;5(1). doi:10.1530/EO-25-0065

10. Sorbye H, Kong G, Grozinsky-Glasberg S, Strosberg J. PRRT in high-grade digestive neuroendocrine neoplasms (NET G3 and NEC). Journal of Neuroendocrinology. John Wiley and Sons Inc; 2025. doi:10.1111/jne.13443 PubMed PMID: 39243213.

11. Hope TA, Allen-Auerbach M, Bodei L, Calais J, Dahlbom M, Dunnwald LK, et al. SNMMI Procedure Standard/EANM Practice Guideline for SSTR PET: Imaging Neuroendocrine Tumors. J Nucl Med. 2023 Feb;64(2):204–10. doi:10.2967/jnumed.122.264860

12. Kwekkeboom DJ, Krenning EP. Somatostatin receptor imaging. Semin Nucl Med. 2002 Apr;32(2):84–91. doi:10.1053/snuc.2002.31022

13. Reccia I, Pai M, Kumar J, Spalding D, Frilling A. Tumour Heterogeneity and the Consequent Practical Challenges in the Management of Gastroenteropancreatic Neuroendocrine Neoplasms. Cancers (Basel). 2023 Mar 20;15(6):1861. doi:10.3390/cancers15061861

14. Chan DL, Pavlakis N, Schembri GP, Bernard EJ, Hsiao E, Hayes A, et al. Dual Somatostatin Receptor/FDG PET/CT Imaging in Metastatic Neuroendocrine Tumours: Proposal for a Novel Grading Scheme with Prognostic Significance. Theranostics. 2017;7(5):1149–58. doi:10.7150/thno.18068

15. Ambrosini V, Campana D, Polverari G, Peterle C, Diodato S, Ricci C, et al. Prognostic Value of ^{68} Ga-DOTANOC PET/CT SUV $_{max}$ in Patients with Neuroendocrine Tumors of the Pancreas. Journal of Nuclear Medicine. 2015 Dec;56(12):1843–8. doi:10.2967/jnumed.115.162719

16. Kratochwil C, Stefanova M, Mavriopoulou E, Holland-Letz T, Dimitrakopoulou-Strauss A, Afshar-Oromieh A, et al. SUV of [^{68}Ga]DOTATOC-PET/CT Predicts Response

Probability of PRRT in Neuroendocrine Tumors. Mol Imaging Biol. 2015 Jun 16;17(3):313–8. doi:10.1007/s11307-014-0795-3

17. Strosberg JR, Al-Toubah T, Haider M, El-Haddad G, Montilla-Soler J. Somatostatin Receptor Expression on [^{68} Ga]Ga-DOTATATE PET Among Patients with Poorly Differentiated Extrapulmonary Neuroendocrine Carcinomas: A Prospective Study. Journal of Nuclear Medicine. 2026 Jun 11;jnumed.125.271460. doi:10.2967/jnumed.125.271460

18. Islam O, Sarti K, Verbruggen L, Vandersmissen V, Bulcke K Vanden, Annys L, et al. Management of high-grade neuroendocrine neoplasms: impact of functional imaging. Endocr Relat Cancer. 2025 Apr 1;32(4). doi:10.1530/ERC-24-0231

19. Singh S, Halperin D, Myrehaug S, Herrmann K, Pavel M, Kunz PL, et al. [^{177}Lu]Lu-DOTA-TATE plus long-acting octreotide versus high-dose long-acting octreotide for the treatment of newly diagnosed, advanced grade 2–3, well-differentiated, gastroenteropancreatic neuroendocrine tumours (NETTER-2): an open-label, randomised, phase 3 study. Lancet. 2024;403(10446):2807–17. doi:10.1016/S0140-6736(24)00701-3

20. Chan DL, Hayes AR, Karfis I, Conner A, Furtado O'Mahony L, Mileva M, et al. Dual [^{68}Ga]DOTATATE and [^{18}F]FDG PET/CT in patients with metastatic gastroenteropancreatic neuroendocrine neoplasms: a multicentre validation of the NETPET score. Br J Cancer. 2023;128:549–55. doi:10.1038/s41416-022-02061-5

Figure legends

Figure 1. Flowchart of the patient cohort.

Figure 2. ^{68}Ga-DOTATOC Krenning score according to SSTR2 IHC status (n = 25). No IHC-negative patient reached a Krenning score of 3–4, whereas 8 of 19 IHC-positive patients scored below 3. p = 0.007 (Cochran–Armitage trend).

Figure 3. SSTR2 IHC score in relation to highest SUVmax on DOTATOC and FDG PET/CT. A) Illustrating the SSTR2 expression score in relation to DOTATOC SUV max (g/ml, log scale) (n = 25). and **B)** in relation to FDG SUV max (g/ml, log scale) (n = 17). For each patient, the highest SUVmax measurement in the primary tumour or metastasis is shown. Each dot symbolizes one patient. Boxes show the median and interquartile range, and whiskers extend to 1.5 × the interquartile range. The y-axes are on a logarithmic scale. DOTATOC uptake increased with SSTR2 expression ($\rho = 0.58$, $p = 0.002$), whereas FDG uptake showed no significant correlation with SSTR2 expression ($\rho = -0.26$, $p = 0.32$).

Figure 4. Dual-tracer phenotypes in patients imaged with both tracers (n = 9). Distribution of individual tumour characteristics based on ^{68}Ga-DOTATOC (Krenning score) and ^{18}F-FDG tracer (Tumour-to-Liver Ratio, TLR) uptake. Thresholds at Krenning 2 and FDG-TLR ≥1.0 define four metabolic phenotypes. The majority (n=7) was Double Positive (SSTR+/FDG+), exhibiting high glucose metabolism alongside maintained receptor expression. Discordant phenotypes were limited to one case: SSTR-/FDG+. One case showed a double negative phenotype.

Figure 5. Discordant SSTR−/FDG+ phenotype in a patient with rectal NEC. Dual-PET imaging and immunohistochemistry imaging; with ^{68}Ga-DOTATOC PET/CT (upper panel: axial CT, fused PET/CT images and axial PET) and ^{18}F-FDG PET/CT (middle panels, axial CT, fused PET/CT images and axial PET) in a 59-year-old patient with NEC. Imaging demonstrating intense FDG uptake in a liver metastasis (orange arrowhead, upper middle panel), followed by disease progression 10 months later (orange arrow upper panel), with no corresponding uptake on DOTATOC PET. The primary rectal tumour (blue arrow, lower middle panel) with intense FDG-uptake.The corresponding routine histology (left) and immunohistochemical staining (right) of the primary rectal tumour (lower panel), demonstrating SSTR2 expression in less than 5% of tumour cells (Grade 0).

Figure 6. Ki-67 index in relation to highest SUVmax per patient regardless of primary tumour or metastasis **A)** ^{68}Ga-DOTATOC (n = 34) and **B)** ^{18}F-FDG PET/CT (n = 23). Each dot represents one patient; the dashed line shows the linear trend with its 95% CI. Y-axes are logarithmic. No significant correlation was found (Spearman $\rho = 0.05$, $p = 0.791$ and $\rho = 0.15$, $p = 0.49$, respectively).

Tables

Table 1. Demographics, tumour characteristics, histopathology and grading, treatment and clinical outcomes, in the cohort.

Characteristic	All Patients (n = 48)
Demographics	
Age, median (range)	72 (37–88)
Sex, n (%)	
Male	30 (62.5%)
Female	18 (37.5%)
Tumour Characteristics	
Primary tumour location, n (%)	
Pancreas	19 (39.6%)
Cancer of unknown primary (CUP)	9 (18.8%)
Rectum	5 (10.4%)
Colon	3 (6.3%)
Anal canal	2 (4.2%)
Esophagus	2 (4.2%)
Gallbladder / biliary tract	2 (4.2%)
Stomach	2 (4.2%)
Duodenum	1 (2.1%)
Small intestine	1 (2.1%)
Prostate	1 (2.1%)
Lower GI (other)	1 (2.1%)
Primary tumour volume (ml), median (range), n = 33	30 (0.6–1137.8)
Histopathology & Grading	
WHO 2022 classification, n (%)	
NET grade 3	13 (27.1%)
NEC	35 (72.9%)
Ki-67 index (%), median (IQR)	70 (44–90)
NET grade 3	28 (24–33)
NEC	80 (67.5–90)
SSTR2 Immunohistochemistry, n (%), n = 34 (70.8%)	
Positive (≥75% expression)	14 (41.2%)
Partial (5 to <75% expression)	12 (35.3%)
Negative (<5% expression)	8 (23.5%)
Circulating Biomarkers, median (IQR)	
Chromogranin A (ng/mL), n = 16	5 (3–34)
5-HIAA (ng/mL), n = 8	171 (78–1004)
CEA (ng/mL), n = 13	2.6 (1.7–8.7)
CA 19-9 (U/mL), n = 16	16 (11–55)
CA 125 (U/mL), n = 9	13 (12–14)

Characteristic	All Patients (n = 48)
Tumour Immunohistochemistry (Positive), n/available (%)	
Chromogranin A	30/33 (90.9%)
Synaptophysin	33/33 (100%)
p53 mutation	10/34 (29.4%)
RB mutation	8/29 (27.6%)
PD-L1	9/18 (50.0%)
Metastatic Sites on Imaging, n (%)	
Liver	35 (72.9%)
Abdominal lymph nodes	29 (60.4%)
Bone	15 (31.3%)
Lung	10 (20.8%)
Brain	7 (14.6%)
Adrenal gland	5 (10.4%)
Peritoneal carcinomatosis	4 (8.3%)
No metastasis	1 (2.1%)
Treatment Regimen, n yes/no (% yes)	
Platinum–etoposide chemotherapy	33/15 (68.8%)
CAPTEM chemotherapy (capecitabine and temozolomide)	31/17 (64.6%)
FOLFIRI chemotherapy (5-fluorouracil, leucovorin and irinotecan)	12/36 (25.0%)
Immunotherapy (PD-L1 inhibitor atezolizumab)	1/47 (2.1%)
Targeted therapy (mTOR inhibitor)	8/40 (16.7%)
PRRT (^{177}Lu-DOTATATE)	10/38 (20.8%)
Clinical Outcomes	
Survival time (months), median (IQR)	20 (11–28)
Deceased at follow-up, n (%)	40 (83.3%)

Data presented as median (range or IQR) for size primary tumour median (range).

CA 19-9 = Cancer Antigen 19-9, CA-125 = Cancer Antigen -125 , CAPTEM = capecitabine and temozolomide CEA = Carcinoembryonic antigen, CUP = cancer of unknown primary, GI=gastrointestinal, IQR= interquartile range, Ki-67=marker cellproliferation , mTOR = mechanistic target of rapamycin, N=number, NEC = neuroendocrine carcinoma, NET= neuroendocrine tumour, p53 = protein 53, PD-L1 = programmed death-ligand 1 , RB1 = retinoblastoma protein 1, PRRT = peptide receptor radionuclide therapy, SSTR2= somatostatin receptor 2, WHO = World Health organization. 5-HIAA= 5-Hydroxyindoleacetic Acid

Additional files

Additional file 1 (.docx): Supplemental Table 1 and Supplemental Figures 1–6.

Supplemental Table 1: biopsy or surgical specimen in relation to the lesions measured on PET/CT, SSTR2 IHC score and Krenning score. Supplemental Figure 1: Bland–Altman plot

of interobserver agreement. Supplemental Figure 2: SSTR2 IHC status by Krenning score category. Supplemental Figure 3: SSTR2 IHC grade by FDG uptake. Supplemental Figure 4: SUVmax per patient in the dual-tracer subgroup. Supplemental Figure 5: heterogeneous dual-tracer uptake in a patient with NET G3. Supplemental Figure 6: overall survival by Krenning score (A), by high versus low SSTR uptake (B) and by FDG SUVmax (C).

Figures

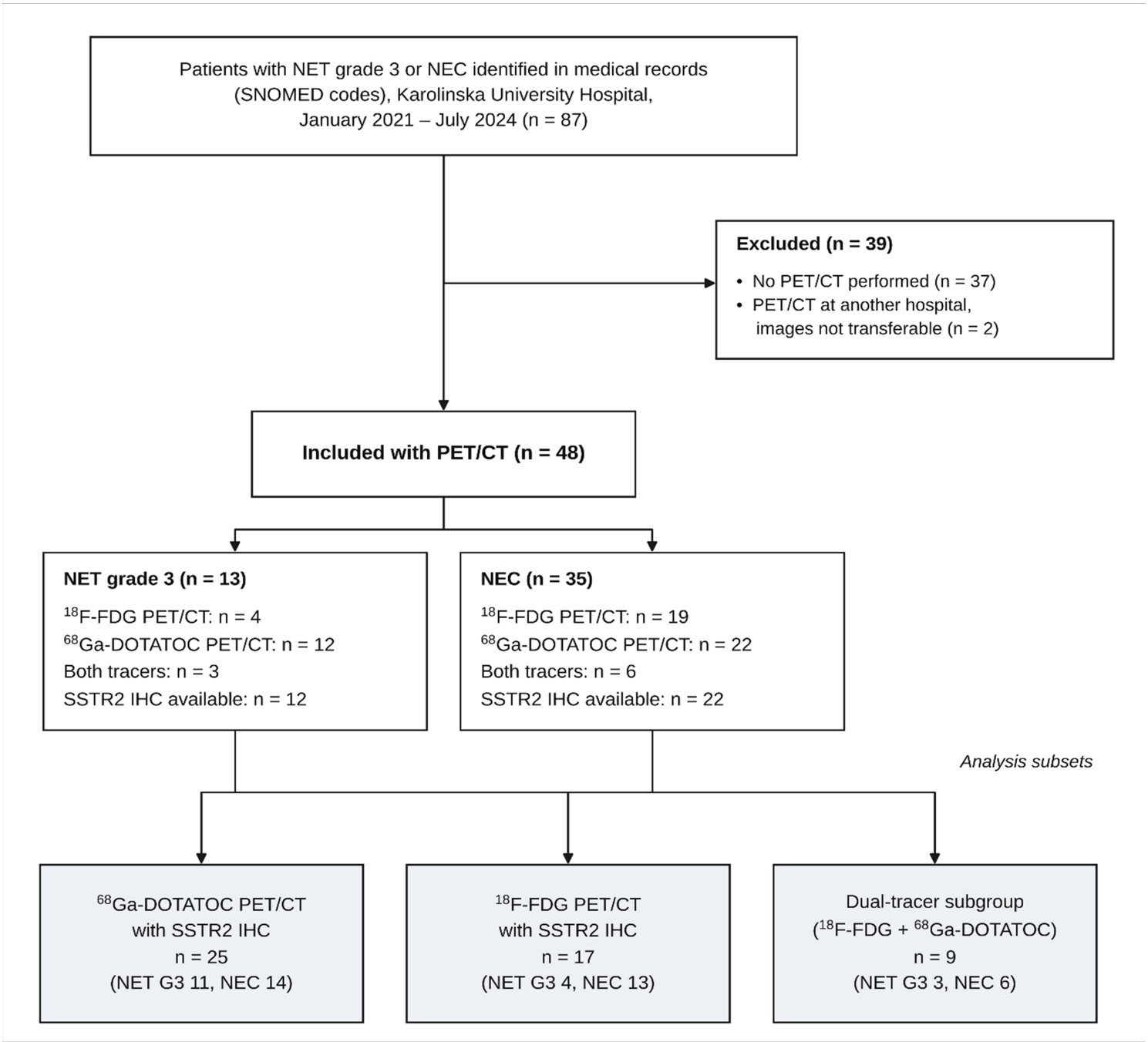


Figure 1

Flowchart of the patient cohort.

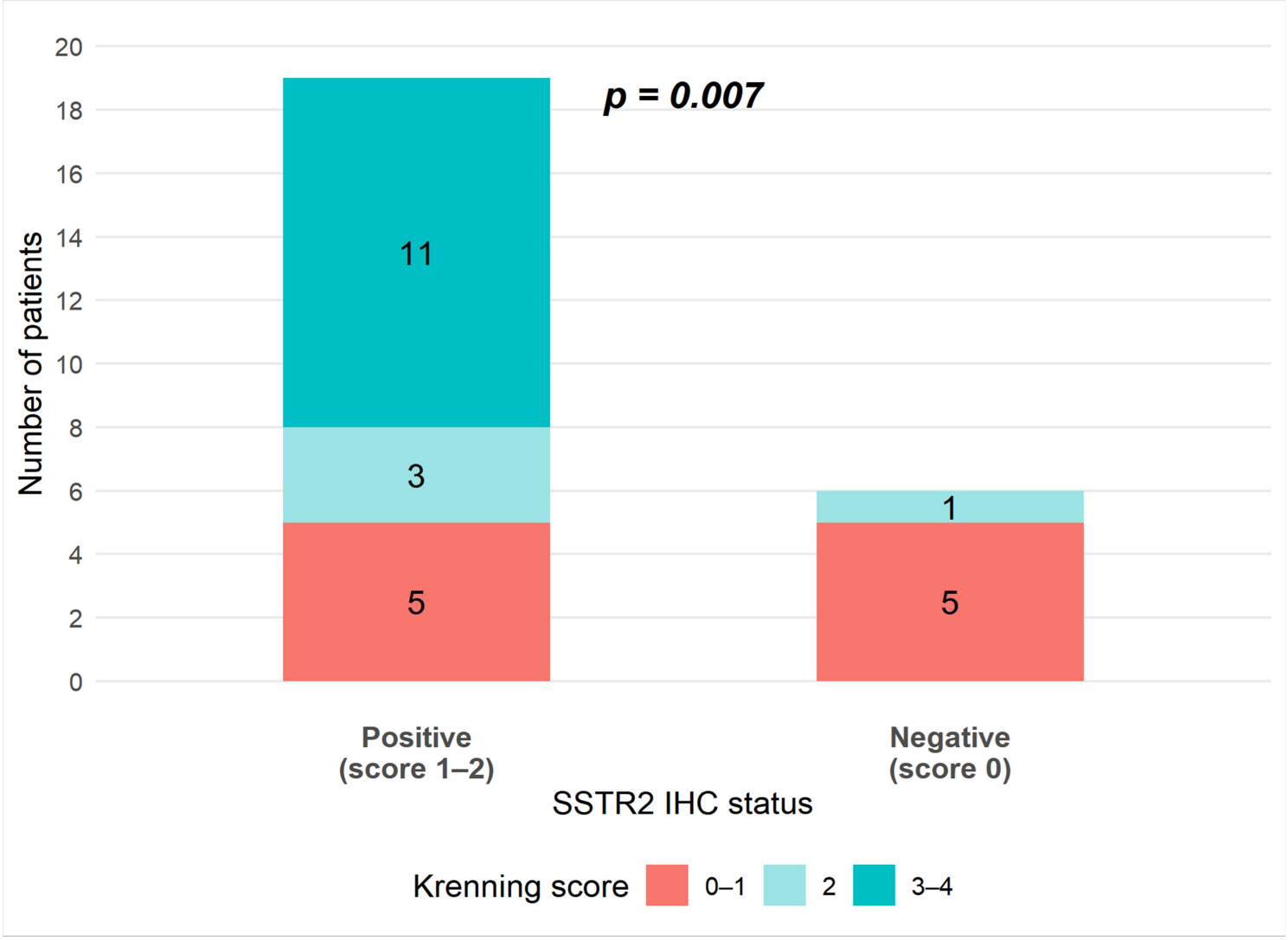


Figure 2

^{68}Ga-DOTATOC Krenning score according to SSTR2 IHC status (n = 25). No IHC-negative patient reached a Krenning score of 3–4, whereas 8 of 19 IHC-positive patients scored below 3. p = 0.007 (Cochran–Armitage trend).

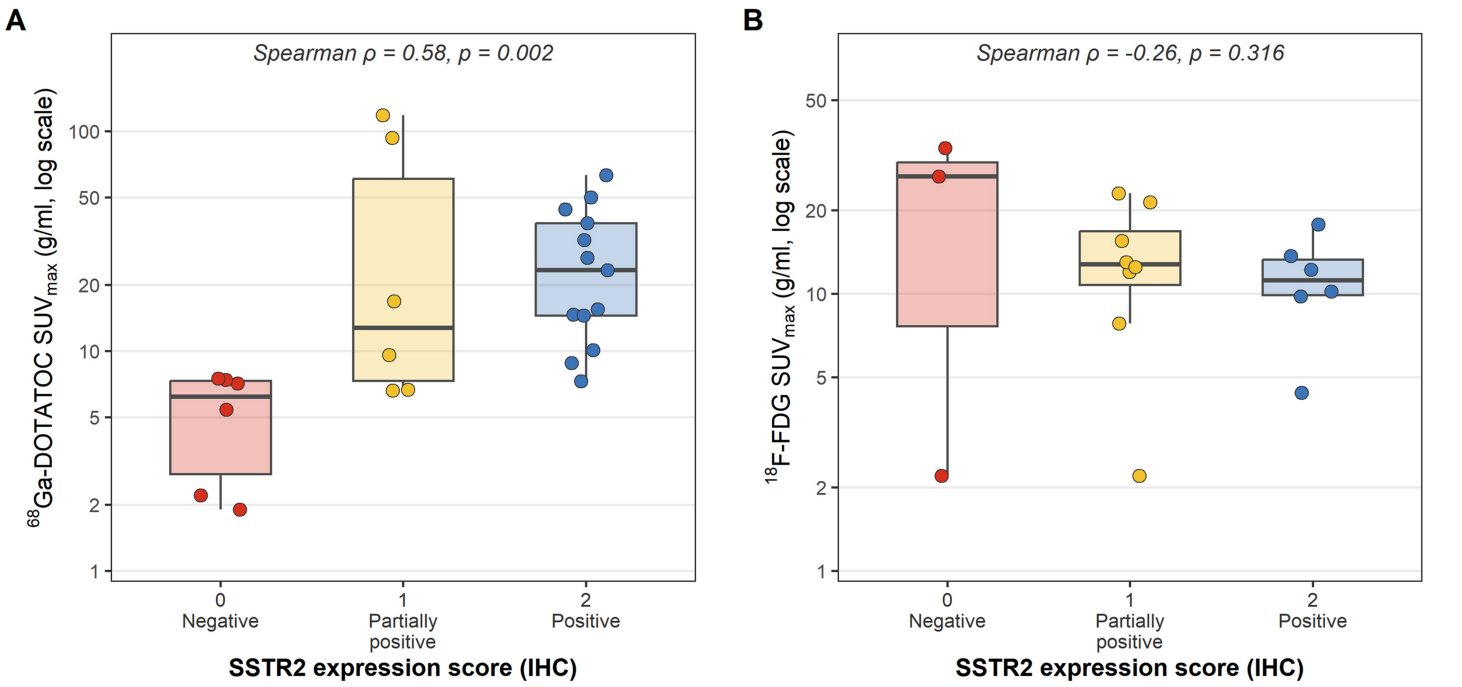


Figure 3

SSTR2 IHC score in relation to highest SUVmax on DOTATOC and FDG PET/CT. A) Illustrating the SSTR2 expression score in relation to DOTATOC SUV max (g/ml, log scale) (n = 25). and**B)** in relation to FDG SUV max (g/ml, log scale) (n = 17). For each patient, the highest SUVmax measurement in the primary tumour or metastasis is shown. Each dot symbolizes one patient. Boxes show the median and interquartile range, and whiskers extend to 1.5 × the interquartile range. The y-axes are on a logarithmic scale. DOTATOC uptake increased with SSTR2 expression (ρ = 0.58, p = 0.002), whereas FDG uptake showed no significant correlation with SSTR2 expression (ρ = −0.26, p = 0.32).

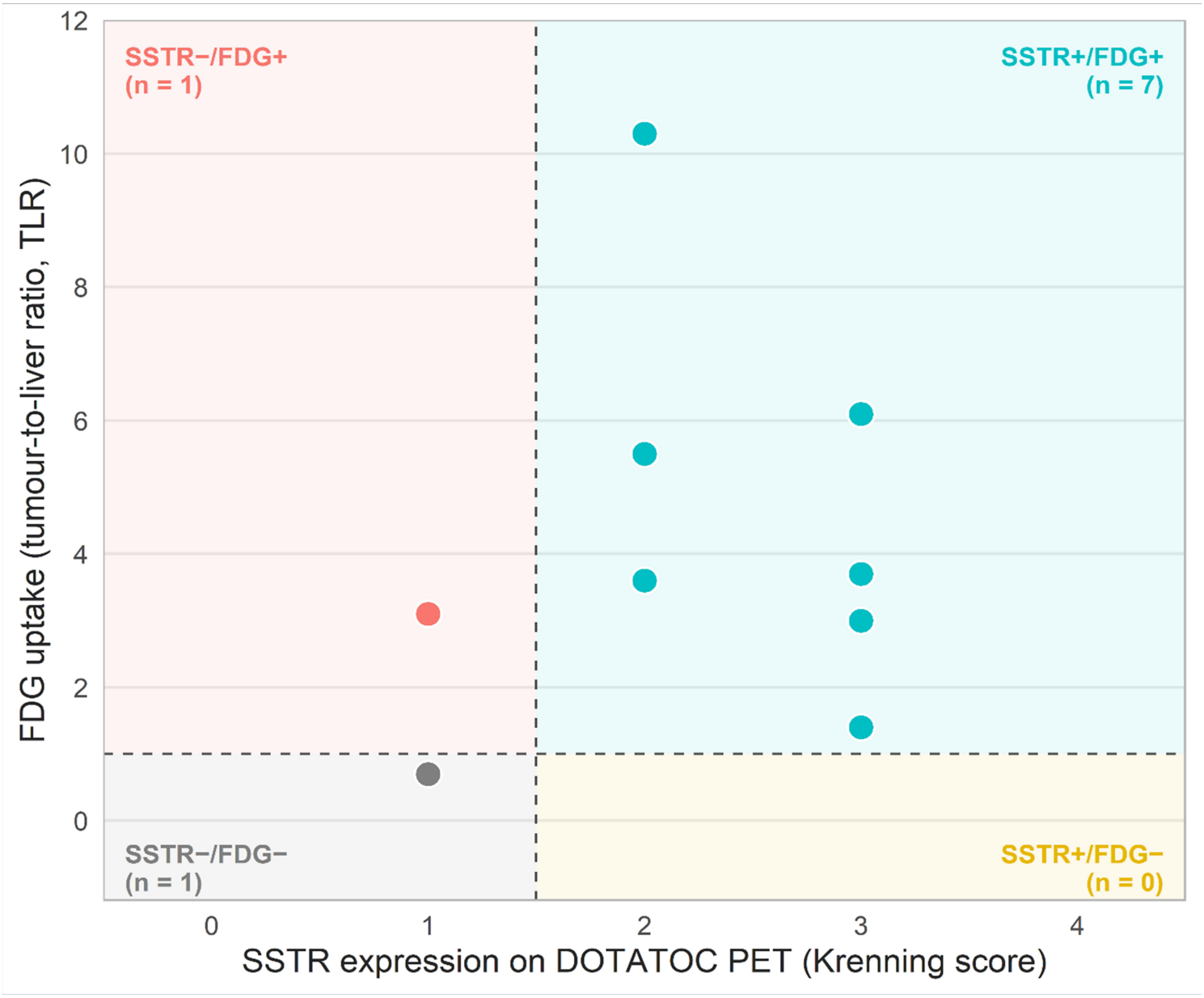


Figure 4

Dual-tracer phenotypes in patients imaged with both tracers (n = 9). Distribution of individual tumour characteristics based on ^{68}Ga-DOTATOC (Krenning score) and ^{18}F-FDG tracer (Tumour-to-Liver Ratio, TLR) uptake. Thresholds at Krenning 2 and FDG-TLR ≥1.0 define four metabolic phenotypes. The majority (n=7) was Double Positive (SSTR+/FDG+), exhibiting high glucose metabolism alongside maintained receptor expression. Discordant phenotypes were limited to one case: SSTR-/FDG+. One case showed a double negative phenotype.

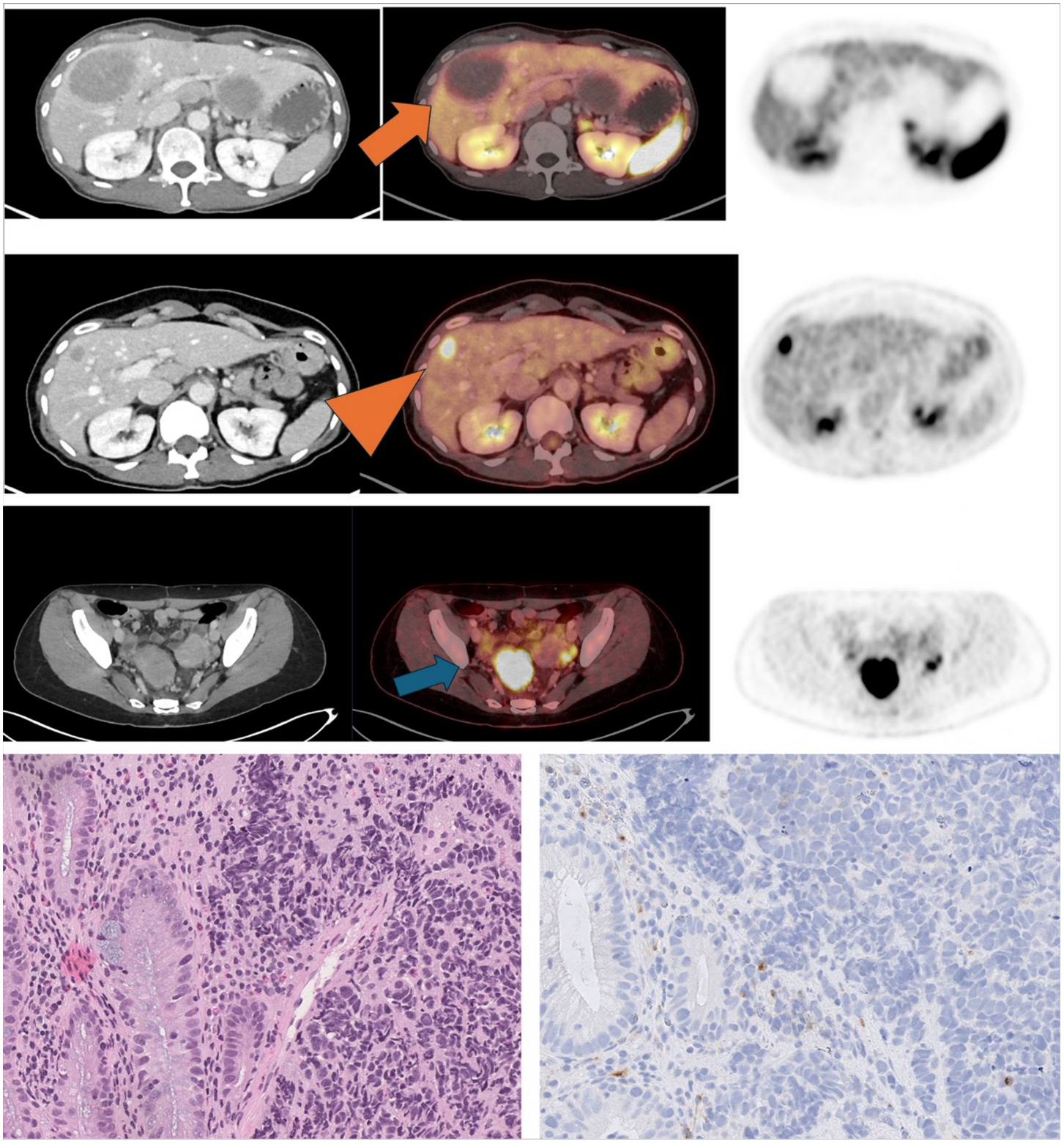


Figure 5

Discordant SSTR−/FDG+ phenotype in a patient with rectal NEC. Dual-PET imaging and immunohistochemistry imaging; with ^{68}Ga-DOTATOC PET/CT (upper panel: axial CT, fused PET/CT images and axial PET) and ^{18}F-FDG PET/CT (middle panels, axial CT, fused PET/CT images and axial PET) in a 59-year-old patient with NEC. Imaging demonstrating intense FDG uptake in a liver metastasis (orange arrowhead, upper middle panel), followed by disease progression 10 months later (orange arrow

upper panel), with no corresponding uptake on DOTATOC PET. The primary rectal tumour (blue arrow, lower middle panel) with intense FDG-uptake.The corresponding routine histology (left) and immunohistochemical staining (right) of the primary rectal tumour (lower panel), demonstrating SSTR2 expression in less than 5% of tumour cells (Grade 0).

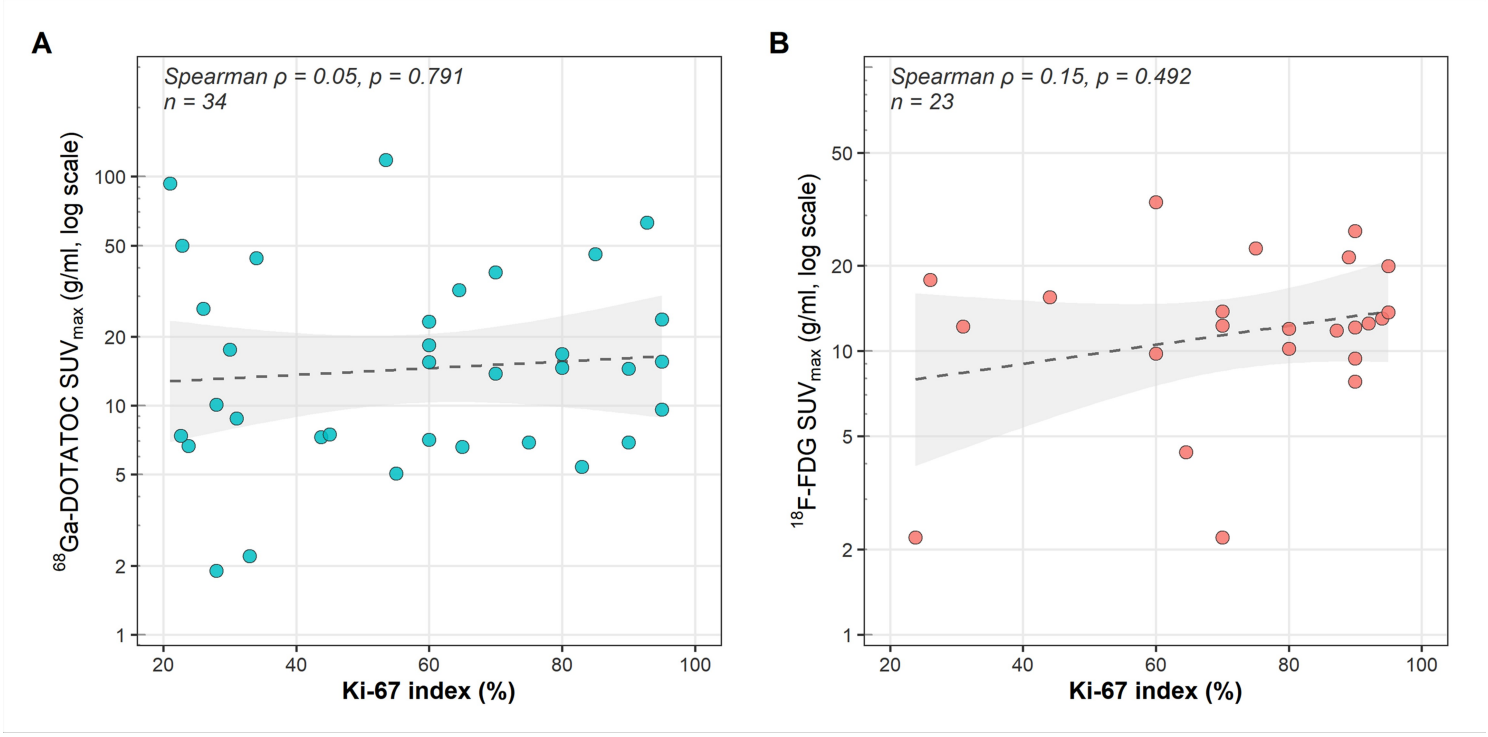


Figure 6

Ki-67 index in relation to highest SUVmax per patient regardless of primary tumour or metastasis **A)** ⁶⁸Ga-DOTATOC (n = 34) and **B)** ¹⁸F-FDG PET/CT (n = 23). Each dot represents one patient; the dashed line shows the linear trend with its 95% CI. Y-axes are logarithmic. No significant correlation was found (Spearman ρ = 0.05, p = 0.791 and ρ = 0.15, p = 0.49, respectively).

Supplementary Files

This is a list of supplementary files associated with this preprint. Click to download.

- TruongSupplementaryEJNMMI.docx